Adipocytes promote pancreatic cancer migration and invasion through fatty acid metabolic reprogramming

ZHIWEI CAI[1,2*], YANG LI[1,2*], MINGJIAN MA[1,2], LONGXIANG WANG[1,2], HONGWEI WANG[1,2], MENG LIU[1,2] and CHONGYI JIANG[1,2]

[1]Department of General Surgery, Huadong Hospital Affiliated to Fudan University; [2]Shanghai Key Laboratory of Clinical Geriatric Medicine, Shanghai 200040, P.R. China

Received November 26, 2021; Accepted May 9, 2023

DOI: 10.3892/or.2023.8578

Abstract. Locally advanced and metastatic pancreatic cancer (PC) frequently grows in adipose tissue and has a poor prognosis. Although adipose tissue is largely composed of adipocytes, the mechanisms by which adipocytes impact PC are poorly understood. Using an *in vitro* coculture model, it was shown that adipocytes promoted tumor progression, and an intricate metabolic network between PC cells and adipocytes was identified and elucidated. First, the proteome of Panc-1 PC cells cultured with or without mature adipocytes was identified. This revealed activated hypoxia signaling in cocultured Panc-1 cells, which was confirmed by the increased expression of factors downstream of hypoxia signaling, such as ANGPTL4 and glycolytic genes, as determined by reverse transcription-quantitative PCR and western blot analysis. In addition, it was demonstrated that coculture with cancer cells activated STAT3 and induced an insulin-resistant phenotype in adipocytes. Furthermore, enhanced fatty acid β-oxidation and increased lipid droplets (LDs) were observed in the cocultured cancer cells. In contrast, downregulated lipid metabolism and a decrease in the size of LDs were found in cocultured adipocytes. Finally, it was shown that the increase in LDs contributed to the increased metastatic capacity of the cocultured PC cells. These data demonstrated that interrupting the mechanisms of lipid uptake from adipocytes in the microenvironment may offer a potential strategy for attenuating PC metastasis.

Correspondence to: Dr Chongyi Jiang, Department of General Surgery, Huadong Hospital Affiliated to Fudan University, 221 West Yan'an Road, Shanghai 200040, P.R. China
E-mail: jiangzhongyi9@sina.com

*Contributed equally

Key words: pancreatic cancer, adipocyte, tumor microenvironment, metabolism, fatty acid

Introduction

Pancreatic cancer (PC) is one of the deadliest cancer types, due in part to a high incidence of early local invasion or distant metastasis (1). During dissemination, cancer cells must adapt to the tumor microenvironment (TME) for successful migration, invasion, and formation of a secondary tumor (2). Various components in the TME act in concert with cancer cells to create a supportive environment during tumor progression (3), making TME-cancer crosstalk an attractive therapeutic target.

Obesity is one of the few known risk factors for PC and correlates with a worse prognosis (4). In accordance with these epidemiological observations, high-fat diets were shown to contribute to tumorigenesis and metastasis in mouse models of PC (5,6). In addition, fatty infiltration in the pancreas is positively associated with the incidence of PC, even after adjusting for confounding factors such as body mass index, indicating the underlying role of obesity in the tumor TME (7). Obesity reportedly can induce an inflammatory and fibrotic microenvironment in PC, resulting in a reduced response to chemotherapy (8). However, among stromal cells in the PC microenvironment, relatively little attention has been given to mature adipocytes, which are closely correlated with obesity.

Adipocytes are the major component of adipose tissue and are a reservoir for energy storage. Adipocytes adjacent to cancer cells show profound phenotypic and functional alterations. (9,10). Using an *in vitro* coculture system, we previously found that adipocytes cocultured with PC cells presented with a delipidation and dedifferentiation phenotype, and these activated cancer-associated adipocytes participated in tumor progression (11). Adipocytes are rich in lipids, the loss of which in cocultured adipocytes may be due to lipid transfer from adipocytes to cancer cells. In breast (12), ovarian (13), and other types of cancer (14,15), adipocyte-derived lipids are a potent energy source that supports cancer growth and progression, suggesting that they may influence cancer metabolism. In the present study, an *in vitro* coculture model was utilized to further interrogate how adipocytes promoted PC progression and to uncover the metabolic interaction between adipocytes and PC cells. The metabolic competitive and energy-plundering relationships between PC cells and adipocytes were identified, where adipocytes showed impaired insulin sensitivity and decreased lipid storage, and PC cells

exhibited enhanced glycolytic capacity and increased the store of lipids. Additionally, the increased levels of lipids in cocultured PC cells contributed to the enhanced metastatic capacity.

Materials and methods

Cells and reagents. The human pancreatic ductal adenocarcinoma cell lines, Panc-1 and Mia PaCa2, were obtained from The Cell Bank of Type Culture Collection of The Chinese Academy of Sciences and were routinely tested for mycoplasma before the experiments. The Panc-1 cells were cultured in DMEM (Gibco; Thermo Fisher Scientific) supplemented with 10% (v/v) FBS (Gibco; Thermo Fisher Scientific). Mia PaCa2 cells were maintained in DMEM supplemented with 10% (v/v) FBS and 2.5% (v/v) horse serum (Gibco; Thermo Fisher Scientific). The murine 3T3-L1 cell line is a well-established cell line that can be stably differentiated into mature adipocytes, and due to its good reproducibility, it is widely used for studies focusing on obesity, diabetes as well as the tumor microenvironment (14,16). Additionally, to the best of our knowledge, there are no stable human preadipocyte or adipocyte cell lines that can be used in such experiments. Thus, murine 3T3-L1 cells were chosen for the present study to ensure the stability of the coculture system, which has been widely used for studies on the crosstalk between cancer cells and adipocytes (14,17). Murine 3T3-L1 preadipocytes were obtained from the American Type Culture Collection and were maintained in DMEM supplemented with 10% newborn calf serum (Gibco; Thermo Fisher Scientific). All cells were cultured in a humidified incubator at 37˚C supplied with 5% CO_2 air. A total of 2 days after reaching confluence, 3T3-L1 cell differentiation was induced by changing the medium to DMEM supplemented with 10% FBS (v/v), 1 μg/ml insulin, 0.5 mM 3-isobutyl-1-methylxanthine, and 1 μM dexamethasone for 2 days. The cells were then incubated in DMEM plus 10% (v/v) FBS and 1 μg/ml insulin for a further 2 days. Next, the differentiated mature adipocytes were cultured in DMEM supplemented with 10% (v/v) FBS. To study the crosstalk process between PC cells and adipocytes, the coculture model was constructed as previously described (11). Briefly, 8 days after induction, the mature adipocytes were cocultured with PC cells in a Transwell indirect coculture system (0.4 μm pore size; Corning, Inc.). Etomoxir (HY-50202, MedChemExpress) was added as a carnitine palmitoyl transferase 1 (CPT1) inhibitor, and CAY10499 (cat. no. 10007875, Cayman Chemical Company) was added as a nonselective lipase inhibitor.

Immunohistochemical staining. The human tissues used in the present study were collected from a 78-year-old female patient with pancreatic ductal adenocarcinoma who underwent radical surgery in Huadong Hospital (Shanghai, China) in March 2019. Consent of the patient and approval from the Institutional Research Ethics Committee of Huadong Hospital, Fudan University (Shanghai, China; approval no. 2018K098) were obtained. Immunohistochemistry was performed as described previously (11). The paraffin-embedded tissues were stained with rabbit anti-FABP4 polyclonal antibody (pAb; cat. no. 12802-1-AP; ProteinTech Group, Inc.) overnight at 4˚C. For each slide, representative images of adipocytes surrounding the normal tissue and adipocytes in the vicinity of the PC cells were obtained. Adipocyte cell sizes were assessed using ImageJ (version 1.8.0; National Institutes of Health).

BODIPY staining of lipid droplets (LDs). To detect LDs in the 3T3-L1 adipocytes, the cells were cultured alone or with cancer cells for 5 days and then incubated in DMEM containing the BODIPY-493/503 lipid probe (0.1 μg/ml, cat. no. D3922, Invitrogen) for 15 min at room temperature. To detect LDs in PC cells treated with 200 μM oleic acid (OA: Beyotime, China), the cells were washed with PBS and fixed with 3.7% paraformaldehyde for 15 min at room temperature. The cells were then incubated with 0.1 μg/ml BODIPY and 5 μg/ml DAPI (Beyotime Institute of Biotechnology) for 15 min at room temperature. The stained cells were visualized using a confocal laser scanning microscope (Olympus) (magnification, x200 or x1,000).

Triglyceride (TG) content analysis. Adipocytes were harvested after being cultured with or without PC cells for 5 days and then lysed with lysis buffer (Beyotime Institute of Biotechnology) for 15 min. The TG content of adipocytes was quantified using a TG assay kit (Applygen Technologies, Inc.). The total protein concentration was measured using a BCA assay (Thermo Fisher Scientific, Inc.), and the results are expressed as milligrams of TG per milligram of protein. The average of the control group was set as one, and all results are presented as the relative TG content.

RNA extraction and reverse transcription-quantitative PCR (RT-qPCR). The cells were harvested and lysed using TRIzol® reagent (Invitrogen; Thermo Fisher Scientific, Inc.) according to the manufacturer's protocol. PrimeScript RT Master Mix (Takara Bio, Inc., cat. no. RR036A) was used to synthesize cDNA according to the manufacturer's protocol. Gene expression was determined using qPCR with a SYBR-Green PCR MasterMix Reagent (Applied Biosystems; Thermo Fisher Scientific, Inc.). The thermocycling protocol consisted of an initial denaturation step at 95˚C for 10 min, followed by 40 cycles of 95˚C for 15 sec and 60˚C for 1 min. All amplifications and detections were performed using an ABI 7500 Real-Time PCR system (Applied Biosystems; Thermo Fisher Scientific, Inc.). Relative gene expression was calculated using the $2^{-\Delta\Delta Cq}$ method with 18S rRNA as an endogenous control (18). The average of the control group was set to one, and all results are presented as the relative mRNA expression. All assays were performed in triplicate. The primer sequences used in the present study are listed in Table I.

Western blotting. Total lysates were extracted using 2% SDS lysis buffer containing phosphatase and protease inhibitors (Roche Diagnostics GmbH). A BCA assay (Thermo Fisher Scientific, Inc.) was used to determine the protein concentration. A total of 20 μg protein was loaded per lane onto 12% SDS-gels, resolved using SDS-PAGE, transferred to 0.22 μm PVDF membranes (MilliporeSigma), and blocked for 1 h at room temperature with 5% skim milk. Each membrane was immunoblotted with the indicated primary antibodies at 4˚C overnight and then incubated with a secondary antibody at 37˚C for 1 h. Immunoreactive bands were visualized using an enhanced chemiluminescence detection kit

Table I. Sequences of the primers used in the present study.

Gene name	Forward primer sequence, 5'-3'	Reverse primer sequence, 5'-3'
18S	CGCCGCTAGAGGTGAAATTCT	CATTCTTGGCAAATGCTTTCG
hANGPTL4	GACCAAGGGGCATGGAGCTT	CAGGGGACCTACACACAACAG
hGLUT1	CTTTGTGGCCTTCTTTGAAGT	CCACACAGTTGCTCCACAT
hHK2	GATTGTCCGTAACATTCTCATCGA	CTTGCAGCAGGGCCAGGCAGTCAC
hLDHA	TGGAGATTCCAGTGTGCCTGTATGG	CACCTCATAAGCACTCTCAACCACC
hFATP1	TGACAGTCGTCCTCCGCAAGAA	CTTCAGCAGGTAGCGGCAGATC
hDGAT1	ACCTCATCTGGCTCATCTTCTTCTA	CCCGGTCTCCAAACTGCAT
hDGAT2	GCTACACTGGCAGGCAACTT	CATTGCCACTCCCATTCTTT
hGPAT4	CCCGTATTTGCTGCTGTTCC	CATACTGCGAGTGCTGAGTGT
hPLIN2	CCTGCTCTTCGCCTTTCG	TGCAACGGATGCCATTTTT
mGLUT4	CCGGATTCCATCCCACAAG	CATGCCACCCACAGAGAAGA
mIRS1	CCAGCCTGGCTATTTAGCTG	CCCAACTCAACTCCACCACT
mSOCS3	GGACCAAGAACCTACGCATCCA	CACCAGCTTGAGTACACAGTCG
mPPARG	CCGAAGAACCATCCGATTGA	TTTGTGGATCCGGCAGTTAAG
mSREBF1	GATGTGCGAACTGGACACAG	GCATGTCTTCGATGTCGTTCAAA
mChREBP	CACTCAGGGAATACACGCCTAC	ATCTTGGTCTTAGGGTCTTCAGG

(Thermo Fisher Scientific, Inc.) using an ImageQuant LAS 4000 System (GE Healthcare). The following primary and secondary antibodies were used in the present study: AKT (1:1,000; ProteinTech Group, Inc.; cat. no. 10176-2-AP), p-AKT^{Ser473} (1:1,000, Cell Signaling Technology, Inc.; cat. no. CST4060S), HIF-1α (1:1,000; ProteinTech Group, Inc.; cat. no. 20960-1-AP), ANGPTL4 (1:1,000; ProteinTech Group, Inc.; cat. no. 18374-1-AP), GLUT1 (1:1,000; ProteinTech Group, Inc.; cat. no. 66290-1-lg), HK2 (1:1,000; ProteinTech Group, Inc.; cat. no. 22029-1-AP), LDHA (1:1,000; ProteinTech Group, Inc.; cat. no. 19987-1-AP), α-tubulin (1:1,000; ProteinTech Group, Inc.; cat. no. 66031-1-lg), p-AMPKα^{Thr172} (1:1,000; Cell Signaling Technology, Inc.; cat. no. CST2535), AMPKα (1:1,000; ProteinTech Group, Inc.; cat. no. 10929-2-AP), p-STAT3^{Tyr705} (1:1,000; Cell Signaling Technology, Inc.; cat. no. CST9145), STAT3 (1:1,000; Cell Signaling Technology, Inc.; CST12640), Snail (1:1,000; CST; CST9782), horseradish peroxidase-conjugated anti-rabbit IgG antibody (1:5,000; ProteinTech Group, Inc.; cat. no. SA00001-2) and goat anti-mouse IgG secondary antibody HRP conjugated (1:5,000; Signalway Antibody LLC; cat. no. L3032).

Migration and invasion assays. For the Transwell migration assay, 5x10^4 Panc-1 or Mia PaCa2 cells in 200 μl DMEM were seeded into the upper chamber of a Transwell chamber with an 8-μm pore membrane (24-well insert; Corning, Inc.). The lower chamber was filled with media supplemented with 10% FBS, while the upper chamber contained serum-free media. Cells were allowed to adhere for 2 h prior to drug treatment and then incubated for 24 h for the migration assays. The cells that had not migrated through the pores were removed using cotton swabs, and the cells on the bottom of the membrane were fixed with 100% methanol and stained with 0.1% crystal violet at room temperature for 30 min. For the invasion assays, the Transwell chambers were coated in advance with 1 mg/ml Matrigel (cat. no. 356231, Corning, Inc.). Cancer cells that invaded through the Matrigel to the underside of the filter were stained with crystal violet at room temperature for 30 min. The number of migrated or invaded cells was counted in three randomly selected fields of view under a brightfield microscope (IX71; Olympus Corporation) (magnification, x100). ImageJ was used to count the number of cells that had migrated or invaded in each field of view.

Lactate assays. After PC cells were either cultured alone or cocultured with adipocytes for 5 days, the conditional medium was collected and centrifuged at 1,000 x g for 5 min at room temperature to remove debris. The supernatants were then stored at -80˚C until required. Lactate released into the medium was measured using the Amplite™ Colorimetric L-Lactate Assay Kit (cat. no. 13815, AAT Bioquest) according to the manufacturer's instructions. Briefly, 50 μl L-Lactate standards and test samples were placed in a white, clear, bottom 96-well microplate. 50 μl L-Lactate working solution was then added to each well of the L-Lactate standard, blank control, and test samples to a final volume of 100 μl/well. The reaction was incubated at room temperature for 2 h in the dark. The absorbance was measured at 575/605 nm. A standard curve based on the absorbance of the L-lactate standards was drawn, and the lactate concentrations in the supernatants were then calculated.

Transmission electron microscopy. PC cells were cultured with or without adipocytes for 5 days. The cells were then collected by centrifugation at 1,000 x g for 10 min at room temperature and immediately fixed in 2.5% glutaraldehyde, 4% paraformaldehyde, and 0.002% picric acid in a 0.1 M (pH 7.3) cacodylate buffer at 4˚C for 3 h. Tissue slices were then postfixed in 1% OsO_4 in the same buffer at 4˚C for 3 h, dehydrated in a graded acetone series, and embedded in Epon resin. For electron microscopy, 70-nm thick sections were cut from tissue resin blocks. The sections were then transferred

to formvar-coated copper mesh grids and double-stained with saturated uranyl acetate for 30 min, followed by lead citrate for 15 min at room temperature. The ultra-thin sections on the grids were examined in a JEOL JEM-1400 plus transmission electron microscope at 80 kV. ImageJ (version 1.8.0; National Institutes of Health) was used to count the number of LDs.

Oxygen consumption rate (OCR) and extracellular acidification rate (ECAR). After culturing with or without adipocytes for 5 days, PC cells were seeded into 96-well plates at a density of 40,000 cells/well and incubated overnight. Mitochondrial function and cellular glycolytic capacity were determined using the Seahorse Bioscience XF96 Extracellular Flux Analyzer (Seahorse Bioscience) and a Seahorse XF Glycolysis Stress Test Kit and a Cell Mito Stress Test Kit, according to the manufacturer's protocol. For ECAR assessment, cells were incubated under basal conditions with non-buffered RPMI 1640 followed by sequential injection of 10 mM glucose and 1 mM mitochondrial poison (oligomycin; MilliporeSigma). OCR was evaluated under basal conditions, followed by a sequential injection of 1 μM oligomycin, 1 μM fluoro-carbonyl cyanide phenylhydrazone (FCCP; MilliporeSigma), and 2 mM antimycin A and rotenone (MilliporeSigma). Both ECAR and OCR measurements were standardized to total protein content.

RNA sequencing (RNA-seq) and gene set enrichment analysis (GSEA). RNA-seq was performed on 3T3-L1 cells cultured with or without Panc-1 PC cells for 5 days as previously described (11). The sequencing data have been deposited in the Gene Expression Omnibus under accession number GSE123939. GSEA was performed using GSEA software (http://www.broadinstitute.org/gsea/index.jsp). A gene set enrichment score (ES) estimating genes from a predefined gene set was calculated using GSEA. The thresholds for significance were set by permutation analysis with 1000 gene-set permutations.

Liquid chromatography coupled with tandem mass spectrometry. Panc-1 PC cells were cultured with or without mature adipocytes for 5 days and then resuspended in an ~8-fold volume of lysis buffer (4% SDS, 100 mM HEPES, pH=7.6) containing a protease inhibitor cocktail and PMSF. The homogenate was sonicated on ice for 30 min. The sample was centrifuged at 25,000 x g for 30 min at 4˚C, and the supernatant was stored at -80˚C. Proteins were reduced in 10 mM DTT for 1 h at 37˚C. Protein samples were then cooled to room temperature (RT). The cysteines were blocked in darkness with 30 mM IAA at 37˚C for 30 min. The extracted protein was mixed in equal amounts according to the groups and then precipitated overnight in acetone. The protein samples were then resuspended in 1 M urea buffer and digested with trypsin overnight. Next, peptides were isotopically labeled with iTRAQ reagents (Applied Biosystems; Thermo Fisher Scientific, Inc.) for 2 h at RT. The labeling reaction was then stopped using water. The samples were then separated and identified using a TripleTOF 4600 mass spectrometer (Applied Biosystems; Thermo Fisher Scientific, Inc.).

Statistical analysis. All statistical analysis was performed using GraphPad Prism version 5.0 (GraphPad Software, Inc.). All results are presented as the mean ± standard deviation of at least three repeats. The differences between two groups were determined using an unpaired two-tailed Student's t-test. Multiple-group comparisons were conducted using one-way analysis of variance (ANOVA) followed by Tukey's post hoc test. $P<0.05$ was considered to indicate a statistically significant difference.

Results

Adipocytes contribute to tumor progression. Although obesity adversely affects the long-term outcomes of patients with PC, the crosstalk between adipocytes and PC cells has not been fully elucidated (19). Immunohistochemical staining of the adipocyte marker FABP4 in human PC tissue demonstrated that adipocytes were present in the TME (Fig. 1A). It was also found that adipocytes directly adjacent to the tumor were smaller in size compared to those further away ($P<0.0001$; Fig. 1B). To assess the role of adipocytes in PC progression, an adipocyte-PC cell coculture system was established (Fig. 1C). Our previous study revealed the significant phenotypic alterations in mature adipocytes induced by pancreatic Panc-1 and MIA PaCa2 cells (11); in the present study, the relationship between adipocytes and PC cells was further explored. 3T3-L1 preadipocytes were differentiated into mature adipocytes and then cocultured with human Panc-1 or MIA PaCa2 cells. It was found that cocultured Panc-1 cells exhibited an elongated mesenchymal morphology compared to monocultured Panc-1 cells, which showed a characteristic epithelial morphology and formed compacted colonies (Fig. 1D). It was also found that PC cells cocultured for 5 days with mature adipocytes had a significantly increased migratory and invasive capacity ($P<0.05$; Fig. 1E and F). Taken together, these data indicated that adipocytes surrounding tumors may have promoted PC progression.

Adipocytes enhance hypoxic signaling in cocultured PC cells. To decipher the potential mechanisms responsible for the increased aggressiveness of cocultured cancer cells, mass spectrometry was used to analyze the protein contents of Panc-1 monocultures and those cocultured with adipocytes for 5 days. GSEA revealed a striking overrepresentation of hallmark database-defined pathways involved in hypoxic signaling in Panc-1 cells cocultured with adipocytes compared to those that were monocultured (Fig. 2A). The majority of the top ten upregulated proteins (Table II) are well-established downstream factors of hypoxic signaling, such as ANGPTL4, ENOG, and LDHA (20-22). Whole proteome bioinformatics analysis also revealed that certain metabolic processes and the epithelial-mesenchymal transition were activated in cocultured tumor cells (Fig. 2A). Based on the protein-protein interaction network associated with the enriched functional pathways of carbohydrate metabolism, tissue morphology, and cancer, it was further confirmed that HIF-1α was activated in the cocultured Panc-1 cells (Fig. 2B). Congruently, there was a robust increase in HIF-1α and its related downstream proteins (SNAIL, ANGPTL4, and glycolytic-associated proteins) in the cocultured tumor cells (Fig. 2C), which was further confirmed by RT-qPCR analysis (Fig. 2E and F). It was also found that lactate production was significantly increased in the

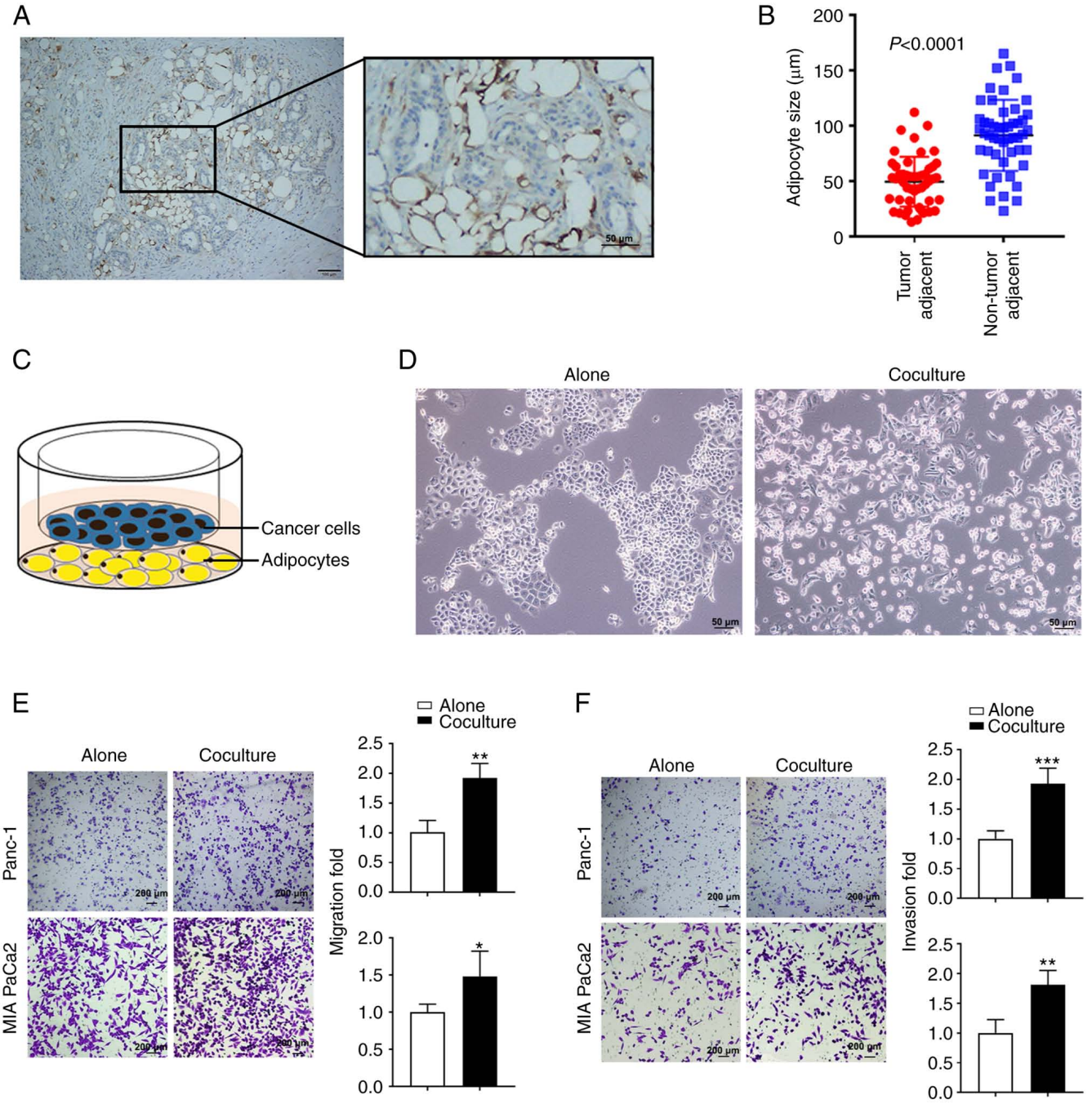

Figure 1. Tumor-neighboring adipocytes promote PC progression. (A) Representative FABP4 staining of adipocytes in the PC tissue. (B) The size of adipocytes adjacent to or distant from pancreatic cancer cells. (C) Schematic illustration of the adipocyte-PC coculture model using a Transwell system. (D) The morphological changes of Panc-1 cells were assessed following coculture with 3T3-L1 mature adipocytes. (E and F) The PC cell lines Panc-1 and MIA PaCa2 were cultured with or without mature adipocytes. After 5 days, cancer cells were used for (E) migration and (F) Matrigel invasion assays. Representative images (left) and quantification (right) of three independent experiments are shown. Data are presented as the mean ± standard deviation. *P<0.05, **P<0.01, ***P<0.001. PC, pancreatic cancer.

cocultured cells (P<0.01; Fig. 2D). Together, these data suggest that adipocytes enhance HIF-1α signaling and can reprogram the tumor metabolic pattern to induce a shift towards anaerobic glycolysis in PC cells under *in vitro* coculture conditions.

PC induces an insulin-resistant phenotype in adipocytes. Given the enhanced ability of glucose utilization in cancer cells, whether coculturing of cells resulted in altered glucose metabolism in adipocytes was next assessed. To address this, RNA-sequencing on mature 3T3-L1 adipocytes cultured alone or with Panc-1 PC cells for 5 days was performed. GSEA of differentially expressed transcripts in cocultured adipocytes compared with those cultured alone revealed a marked enrichment of gene sets corresponding to the insulin signaling pathway and the JAK-STAT3 pathway (Fig. 3A). In addition, there was a robust decrease in genes associated with the insulin signaling pathway in cocultured adipocytes (Fig. 3B), indicating insulin resistance in the adipocytes. It was also found that coculturing the adipocytes with cancer cells increased STAT3 phosphorylation (Fig. 3C). Additionally, the increased phosphorylation

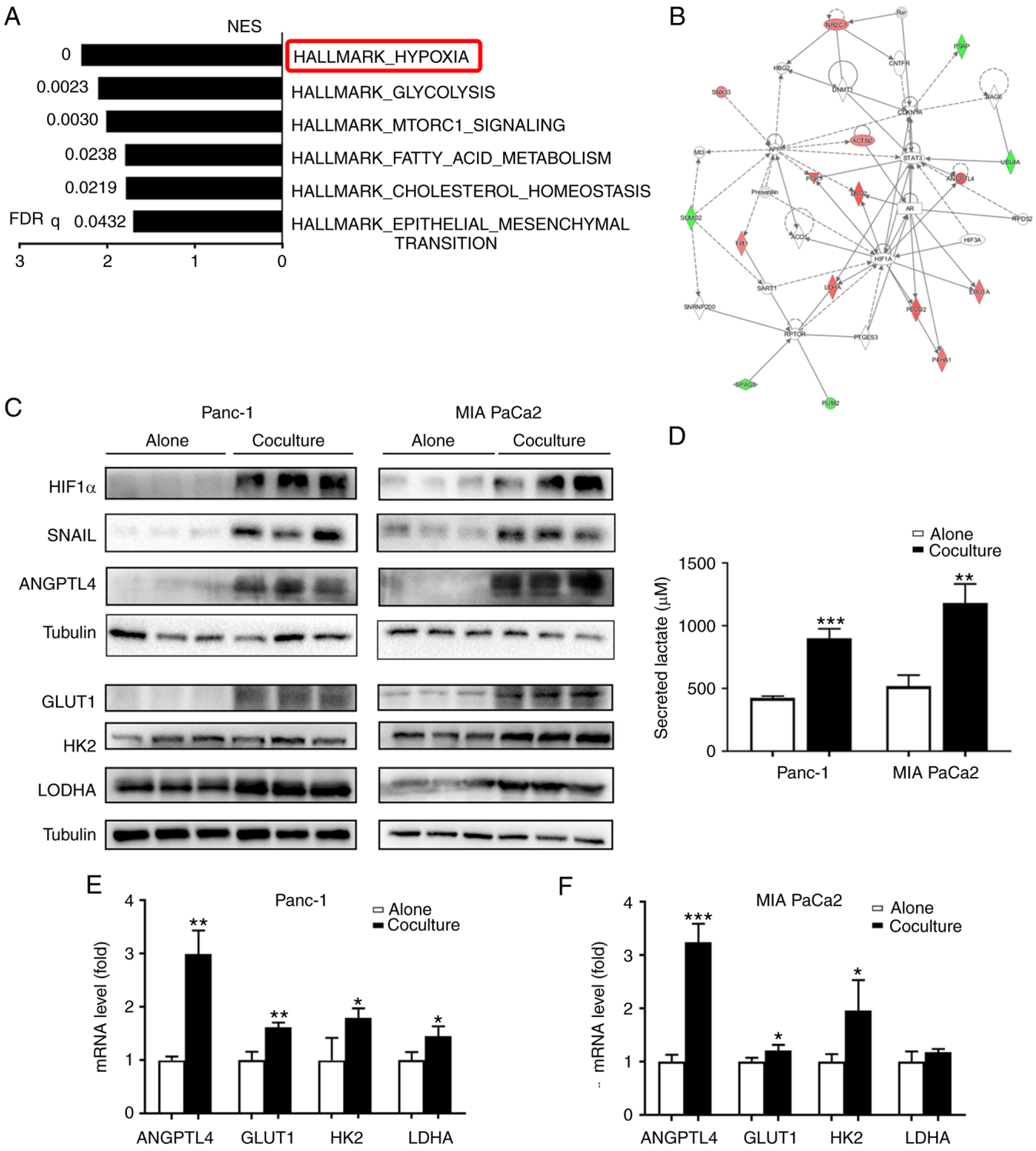

Figure 2. Adipocytes enhance HIF-1α signaling in cocultured pancreatic cancer cells. (A) The top pathways from GSEA of differential expression proteins in Panc-1 cells cocultured with adipocytes vs. monoculture (n=3) using the GSEA Hallmark database. (B) Visualization of the protein-protein interaction network associated with the enriched functional pathways of Carbohydrate Metabolism, Tissue Morphology, and Cancer enriched from differentially expressed proteins in the Panc-1 cells cocultured with adipocytes vs. monoculture (n=3). Gene products are denoted as nodes and the relationships between two nodes as a line. Red and green designate up- and downregulation, respectively. Genes with no coloring were added from the ingenuity knowledge database. (C) Immunoblot analysis of proteins associated with HIF-1α signaling in Panc-1 or MIA PaCa2 cultured with or without adipocytes for 5 days. (D) Analysis of lactate secretion by Panc-1 and MIA PaCa2 cells cultured alone or with adipocytes for 5 days (n=3). (E and F) mRNA expression of ANGPTL4, GLUT1, HK2, and LDHA in levels Panc-1 or MIA PaCa2 when cultured alone or cocultured with mature adipocytes. Data are presented as the mean ± standard deviation. *P<0.05, **P<0.01, ***P<0.001. GSEA, Gene Set Enrichment Analysis.

of STAT3 in adipocytes treated with 20 ng/ml IL-6 resulted in the downregulation of genes related to the insulin signaling pathway, such as GLUT4 and IRS1 (P<0.05; Fig. 3D and E). In humans, SOCS3 expression has been shown to be associated with the JAK-STAT3 pathway and insulin resistance (23). In line with this, significantly increased SOCS3 expression in

Table II. Top ten upregulated proteins in Panc-1 cells cocultured with adipocytes compared with the monocultured cells.

Protein name	Gene name	Fold change	P-value
Solute carrier family 2, facilitated glucose transporter member 1	SLC2A1	2	<0.0001
Angiopoietin-related protein 4	ANGPTL4	1.75	0.00012
Procollagen-lysine,2-oxoglutarate 5-dioxygenase 2	PLOD2	1.655172	0.000685
γ-enolase	ENOG	1.642857	0.00022
Phosphoglycerate kinase 1	PGK1	1.6	0.003857
Vitronectin	VTNC	1.586207	0.003858
Dynein heavy chain 5, axonemal	DYH5	1.560976	0.028439
NFX1-type zinc finger-containing protein 1	ZNFX1	1.56	0.024896
Hemoglobin subunit alpha	HBA	1.535714	0.00257
L-lactate dehydrogenase A	LDHA	1.5	0.584963

adipocytes treated with IL-6 or cocultured with Panc-1 or MIA PaCa2 PC cells was observed (P<0.001; Fig. 3F). Given the close relationship between the JAK-STAT3-SOCS3 axis and the development of obesity-associated disorders, such as insulin resistance (24), it was hypothesized that PC cells could induce an insulin-resistant phenotype in adipocytes through the JAK-STAT3-SOCS3 axis.

Adipocytes alter PC cell fatty acid metabolism. Next, both the ECAR and OCR were measured in PC cells using a Seahorse assay. After monoculture or coculture with 3T3-L1 adipocytes for 5 days, the PC cells were digested and seeded into 96-well plates for further tests. It was found that the ECAR did not differ significantly between the two conditions, indicating no alteration in the rate of glycolysis in PC cells after coculture with adipocytes (Fig. 4A and B). In contrast, the cocultured cancer cells underwent significantly increased OCR in both basal and maximal-uncoupled states compared with monocultured cancer cells (Fig. 4C and D), suggesting enhanced fatty acid β-oxidation (FAO) in the cocultured cancer cells. In cancer, the JAK-STAT3 pathway regulates lipid metabolism through FAO (25), and AMPK favors energy-producing processes by activating β-oxidation (26). Congruently, the presence of mature adipocytes increased STAT3 and AMPK phosphorylation and decreased AKT phosphorylation (Fig. 4E). As adipocytes store LDs, it was hypothesized that adipocytes provide lipids to cancer cells to enhance their FAO ability. To explore the changes in lipids in cocultured PC cells, electron microscopy was performed. The results showed there was a substantial increase in the number of LDs in the cocultured Panc-1 and MIA PaCa2 cancer cells compared with that in the monocultured cells (P<0.05; Fig. 4F and G). Substantial changes in the mitochondrial ultrastructure in the cocultured MIA PaCa2 cells were also observed (Fig. 4G), suggesting enhanced respiratory chain activity in cancer cells after coculture with adipocytes. Taken together, these results showed that adipocytes resulted in increased lipid content and metabolic reprogramming in PC cells.

Increased levels of LDs promote the invasion of cocultured PC cells. The above data showed that during coculture, adipocytes stimulated increased invasiveness and enhanced FAO in PC cells. Thus, whether the utilization of stored lipids in cancer cells was associated with tumor malignancy was further examined. Etomoxir can inhibit CPT1, which serves as the primary rate-limiting factor in the transport of fatty acids to the mitochondria.

First, cancer cells were cocultured with or without adipocytes for 5 days with the addition of etomoxir and then the cancer cells' invasive ability was assessed. It was found that the inhibition of FAO by etomoxir during coculture did not hamper the invasive ability of the cocultured cancer cells, in agreement with the unchanged OCR (Fig. 5A and B). As catabolism of stored LDs promotes cancer invasion and migration (27), whether excess stored lipids contributed to the increased invasive ability of cocultured PC cells compared with monocultures was assessed. Treating the cancer cells with etomoxir to inhibit FAO or with CAY10499 to inhibit lipolysis during the invasion assay significantly reduced the invasion of the cocultured PC cells (P<0.01; Fig. 5C and D). These data indicate that the accumulation of LDs during tumor cell coculture with adipocytes and the utilization of excess lipids during the process of tumor metastasis together resulted in the increased invasive ability of the cocultured PC cells. In agreement with the increased levels of LDs in cocultured cancer cells (Fig. 4F and G), it was also shown that the fatty acid transporter-related gene (FATP1) and lipid storage-related genes (DGAT1, DGAT2, GPAT4, and PLIN2) were upregulated in the cocultured PC cells (Fig. 6A and B), suggesting that coculture with adipocytes promoted fatty acid uptake and storage in the cancer cells. To further confirm this, Panc-1 and MIA PaCa2 cancer cells were first pretreated with exogenous OA, which resulted in lipid accumulation (Fig. 6C and D). Preloading exogenous LDs increased cancer cell aggressiveness, and this effect was abrogated by etomoxir or CAY10499 treatment (P<0.01; Fig. 6E and F). Taken together, these data demonstrated that the presence of adipocytes increased the metastatic capacity of the PC cells, and this was largely due to LD accumulation in the cocultured tumor cells.

PC cells induce downregulated lipid metabolism in cocultured adipocytes. The above data indicated that adipocytes altered PC cell lipid metabolism. Next, whether coculturing with cancer cells also influenced the lipid metabolism of

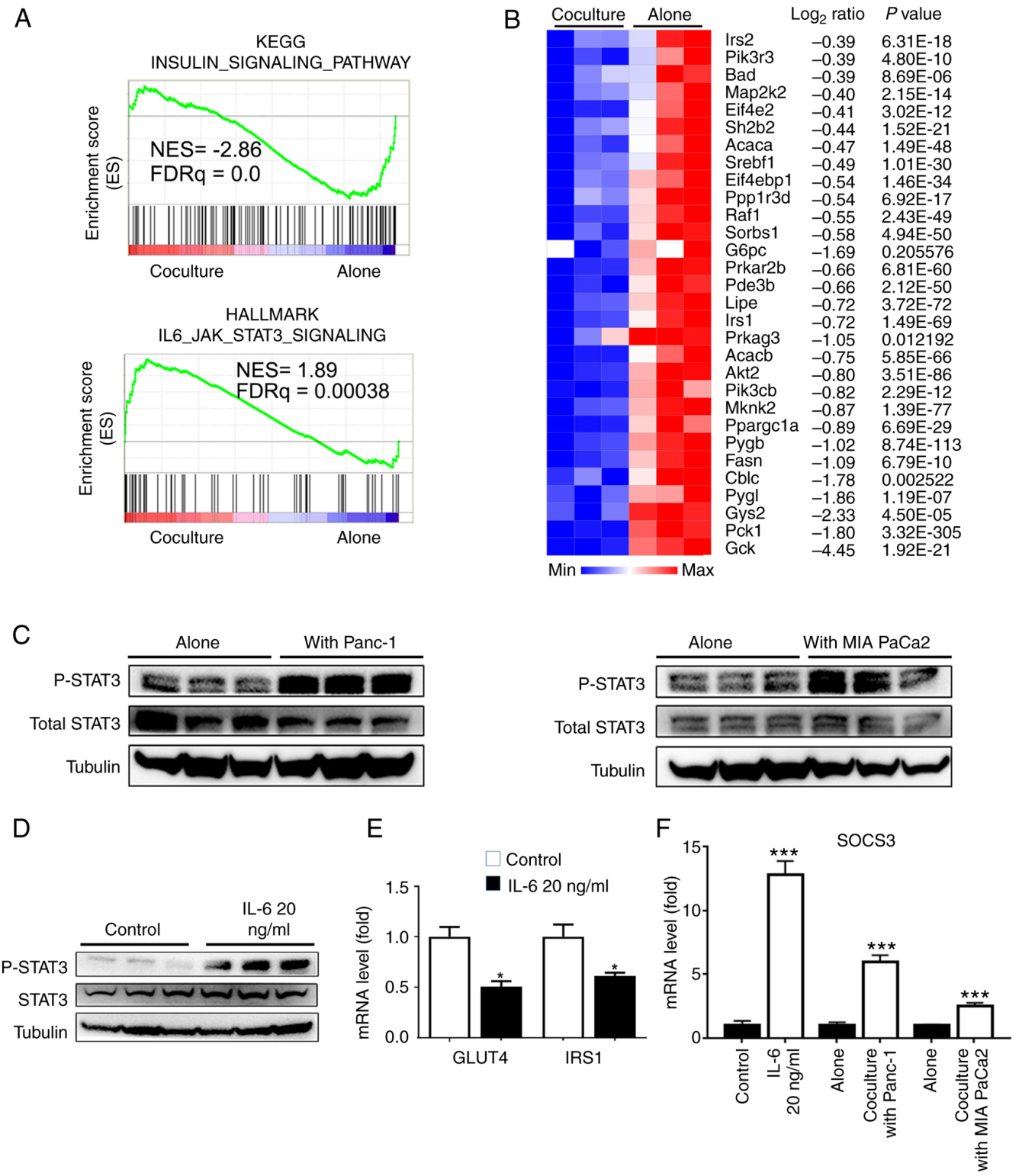

Figure 3. PC cells induce an insulin-resistant phenotype in cocultured adipocytes. (A) Gene Set Enrichment Analysis plots of enrichment in 'KEGG_ Insulin_signaling_pathway' (up), 'HALLMARK_IL6_JAK_STAT3_signaling' (down) signatures in adipocytes cultured with or without cancer cells (n=3). (B) Leading-edge genes of insulin signaling pathway signature described in (A). Red indicates upregulation, and blue indicates downregulation. (C) Immunoblots of total and p-STAT3 in adipocytes cultured alone or with Panc-1 (left) and MIA PaCa2 for 5 days. (D and E) Immunoblot analysis of (D) p-STAT3 and (E) qPCR analysis of insulin signaling genes in 3T3-L1 mature adipocytes treated with IL-6 (20 ng/ml) in medium containing 10% FBS for 48 h. (F) qPCR analysis of SOCS3 expression changes in adipocytes treated with IL-6 (20 ng/ml) or cocultured with Panc-1 and MIA PaCa2 PC cells. Data are presented as the mean ± standard deviation. *P<0.05, ***P<0.001. PC, pancreatic cancer; qPCR, quantitative PCR.

adipocytes was assessed. First, a decrease in the size of LDs was found in cocultured adipocytes, which was consistent with the reduced TG content (P<0.01; Fig. 7A and B). The GSEA of transcripts that were downregulated in the cocultured adipocytes showed enrichment in gene sets corresponding to oxidative phosphorylation, adipogenesis, and

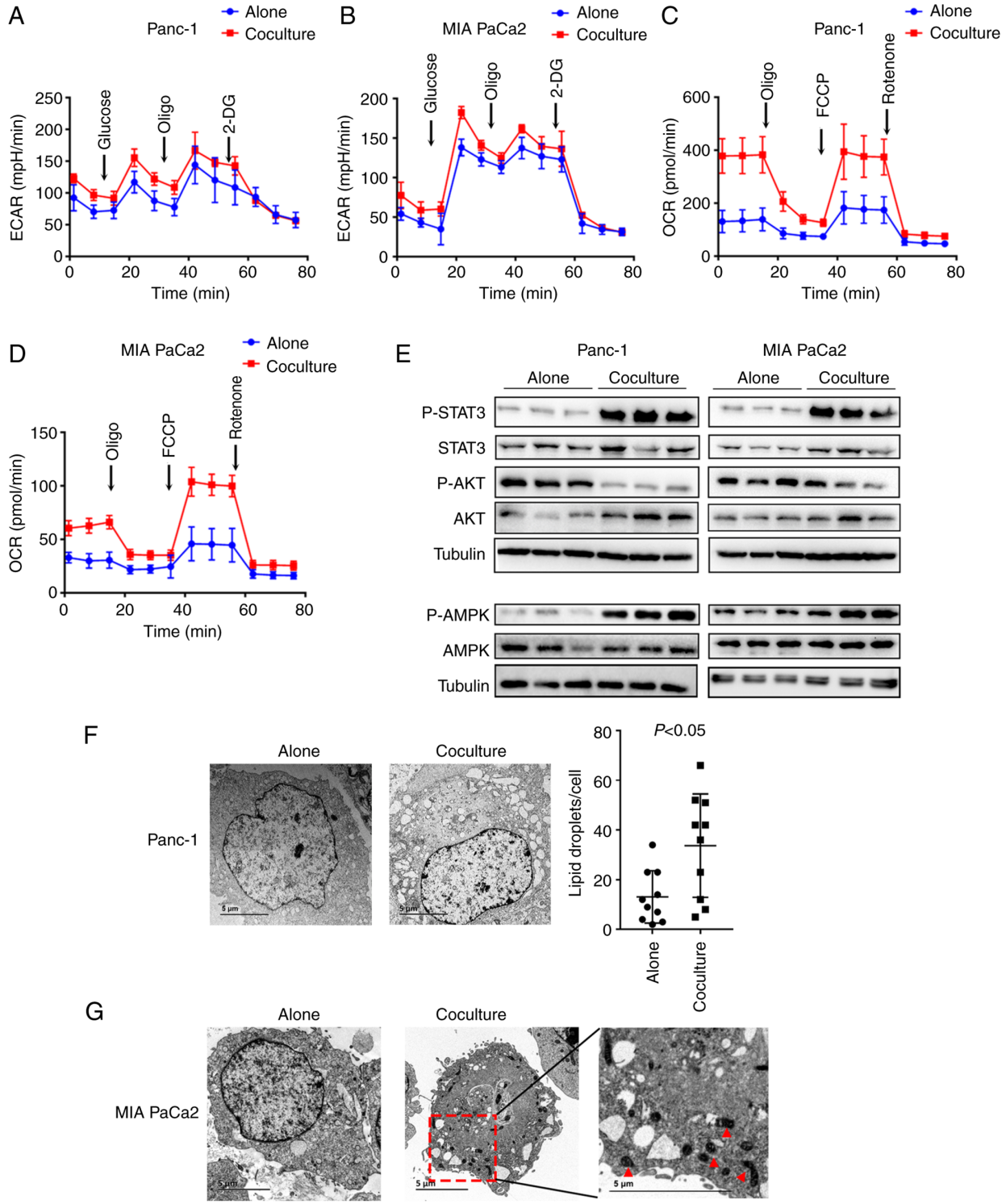

Figure 4. Adipocytes alter pancreatic cancer cell fatty acid metabolism. (A and B) ECAR did not differ between Panc-1 and MIA PaCa2 cancer cells cultured with or without mature adipocytes for 5 days. ECAR was measured under basal conditions followed by the sequential addition of 10 mmol/l glucose, 1 mmol/l oligomycin, and 100 mmol/l 2-deoxy-glucose. (C and D) OCR differed between Panc-1 and MIA PaCa2 cancer cells cultured with or without mature adipocytes for 5 days. OCR was measured under basal conditions followed by the sequential addition of oligomycin (1 μM), FCCP (2 μM), and rotenone (1 μM). (E) Immunoblots of total and p-STAT3, AKT, and AMPK in Panc-1 and MIA PaCa2 cancer cells cultured with or without mature adipocytes for 5 days. (F) TEM of Panc-1 cancer cells cocultured with mature adipocytes for 5 days compared to cells cultured alone as the control (left). Quantification of total lipid droplets per cell is shown (right). n=10 cells/condition. (G) TEM of MIA PaCa2 cells cultured with or without mature adipocytes for 5 days. The red arrows highlight the ultrastructural changes of the mitochondrial in the cocultured cancer cells. ECAR, extracellular acidification rate; OCR, oxygen consumption rate; TEM, transmission electron microscopy; Oligo, oligomycin.

fatty acid metabolism. Further analysis using Gene Ontology and biological process compilation confirmed that both fatty acid catabolic and anabolic processes were suppressed in cocultured adipocytes (Fig. 7C). The GSEA of transcripts that were downregulated in the cocultured adipocytes also revealed marked enrichment of gene sets associated with

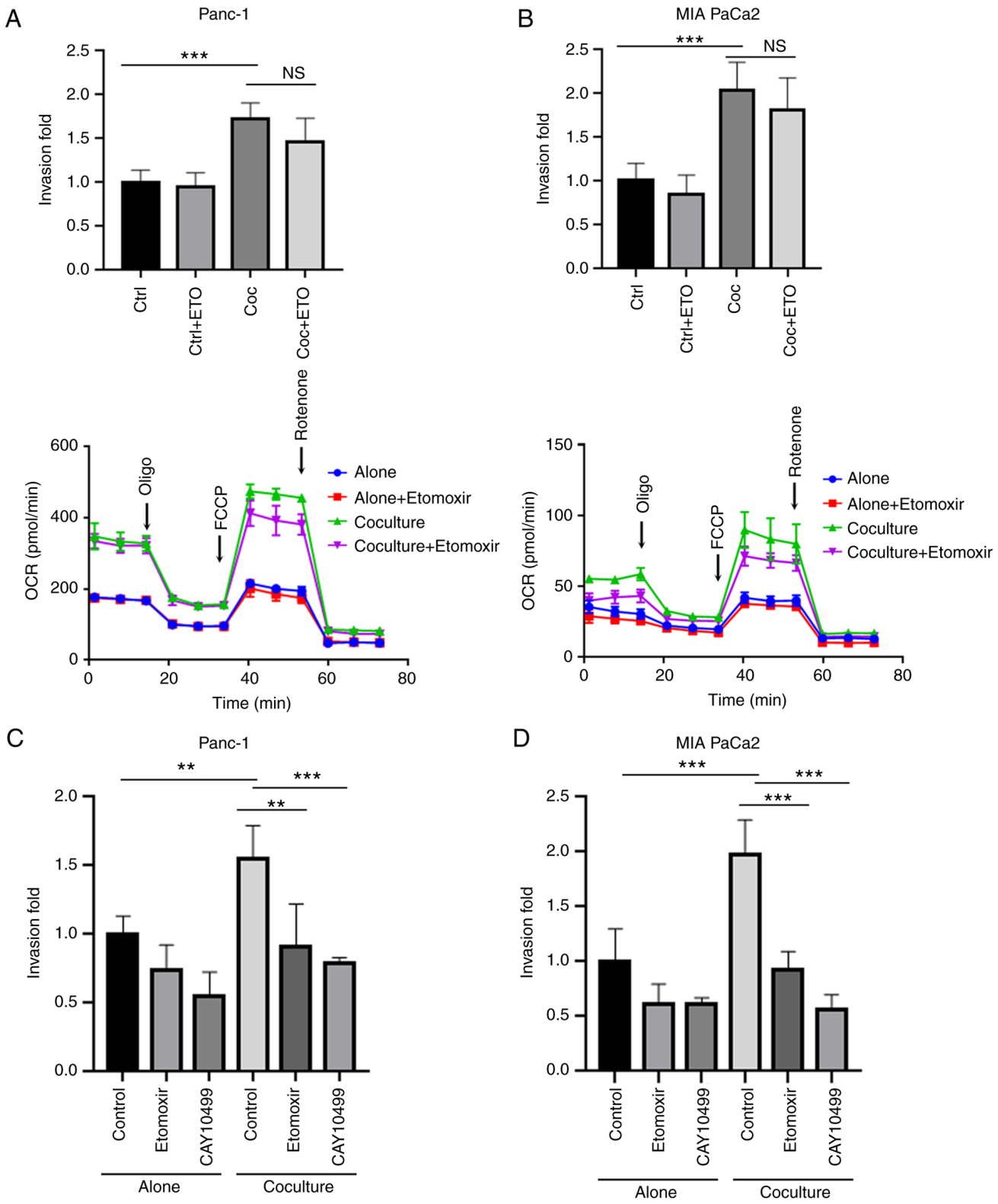

Figure 5. Lipid accumulation in cocultured PC cells promotes cell invasion. (A and B) Transwell invasion of Panc-1 and MIA PaCa2 PC cells when cultured alone or after coculture with mature adipocytes for 5 days with or without pretreatment of 50 μM etomoxir. (C and D) Mitochondrial respiration of Panc-1 and MIA PaCa2 cancer cells cultured with or without mature adipocytes for 5 days, with or without pretreatment of 50 μM etomoxir. (D and E) Quantification of invasion of monocultured or cocultured Panc-1 and MIA PaCa2 PC cells, with or without pretreatment with etomoxir or CAY10499 during the assays. Data are presented as the mean ± standard deviation. **P<0.01, ***P<0.001. NS, not significant; PC, pancreatic cancer; Ctrl, control; Coc, coculture; ETO, etomoxir; Oligo, oligomycin.

adipogenesis (Fig. 7D). In agreement with this, RT-qPCR analysis of the adipocytes revealed the reduced expression of key upstream genes of adipogenesis when cocultured with PC cells (Fig. 7E). Taken together, these results indicate that PC cells downregulated lipid metabolism and adipogenesis in the cocultured adipocytes.

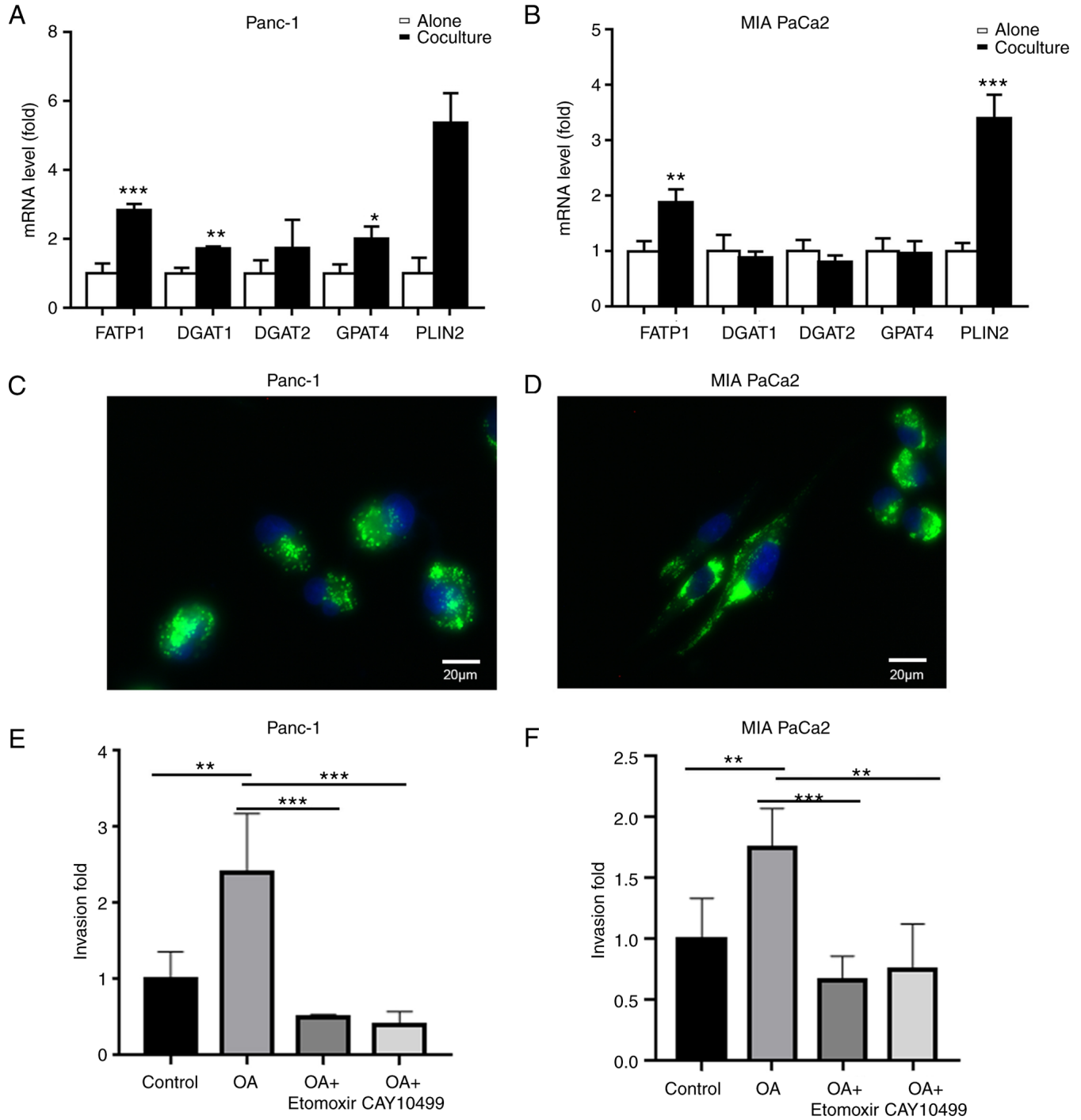

Figure 6. Excess lipid promotes pancreatic cancer cell invasion through lipolysis. (A and B) mRNA expression of FATP1, DGAT1, DGAT2, and PLIN2 in Panc-1 or MIA PaCa2 in the presence or absence of mature adipocytes for 5 days. (C and D) OA-loaded (200 μM) Panc-1 and MIA PaCa2 cancer cells were visualized by staining with BODIPY. (E and F) Quantification of invasion of control or OA-treated Panc-1 and MIA PaCa2, with or without etomoxir and CAY10499 treatment during the assays. Data are presented as the mean ± standard deviation. *P<0.05, **P<0.01, ***P<0.001. OA, oleic acid; LD, lipid droplet.

Discussion

Clinical epidemiological observations and mechanistic research are increasingly establishing the importance of obesity in PC (4,5). However, the underlying mechanisms by which excessive adiposity contributes to tumor progression remain unclear. Adipose tissue as a reservoir for energy storage is closely associated with the pathophysiological process of obesity. An increasing number of studies have indicated that crosstalk exists between adipocytes and cancer cells in the TME. This crosstalk involves a vicious cycle in which adipocytes are activated by cancer cells, and in turn, cancer-associated adipocytes promote tumor progression (28). Altered cellular metabolism is an important feature of cancer cells that enables unrestricted growth and motility. Malignant cells tend to rewire their metabolic properties according to the altered challenges encountered in the TME (29). In breast (12), ovarian (30), and other types of cancer (14,15,31), an increasing

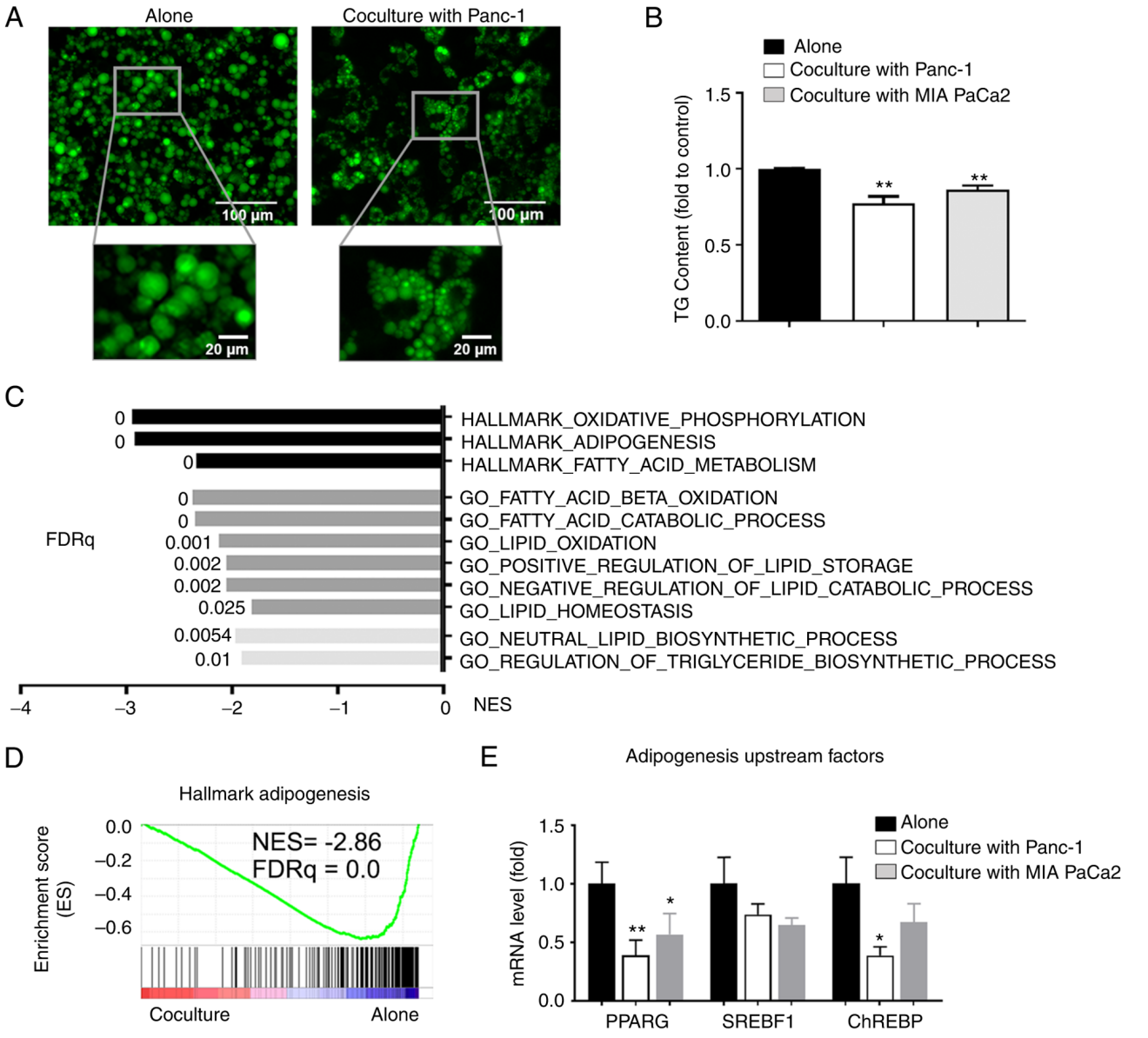

Figure 7. PC cells downregulate lipid metabolism in cocultured adipocytes. LD levels in adipocytes cultured alone or cocultured with PC cells, (A) shown after staining with BODIPY, the size of LDs in cocultured adipocytes decreased, or (B) by measure of TG content, the content of TG in cocultured adipocytes decreased. (C) Top metabolic pathways from GSEA of downregulated genes in adipocytes cocultured with Panc-1 cancer cells (n=3) using GSEA Hallmark and GO biological process MSigDB database. (D) Gene Set Enrichment Analysis plot of enrichment in 'Hallkmark_Adipogenesis' signature in adipocytes cocultured/alone as described in (C). (E) Reverse transcription-quantitative PCR analysis of adipogenesis upstream genes in adipocytes under the indicated conditions. Data are presented as the mean ± standard deviation. *P<0.05, **P<0.01. PC, pancreatic cancer; LD, lipid droplet; TG, triglyceride; FDRq, false discovery rate, q value.

number of studies have revealed that tumor metabolic crosstalk with adipocytes contributes to tumor metastasis. In this study, an intricate metabolic network that contributes to the anabolic reprogramming of cancer cells and favors tumor aggressiveness was revealed between PC cells and adipocytes.

First, a metabolic competitive relationship between PC cells and adipocytes was revealed, where PC cells subverted adipocyte glucose utilization by desensitizing adipocytes to glucose. Diabetes is a well-known risk factor for PC, and PC also seems to cause glucose intolerance (32). Certain clinical studies have shown that PC-related diabetes is improved following tumor resection (33,34). In line with this, intraperitoneal injection of PC cell-conditioned media into immunodeficient mice resulted in significantly diminished glucose tolerance compared with controls injected with saline (35). These studies together suggest that PC can cause glucose desensitization of normal tissues. The ability of tumors to impair adipocyte insulin sensitivity could serve to divert insufficient nutrients in the TME. Thus, it was hypothesized that in the pancreatic TME with limited glucose, PC cells may induce a diabetic state to obtain a competitive advantage for the acquisition of glucose. Indeed, it was found that coculturing with adipocytes induced an increase in glycolytic capacity in PC cells through the upregulation of glycolytic enzymes.

Most tumors utilize enhanced glucose metabolism to sustain anabolic processes, which is often related to a more hypoxic tumor signature (36). The pancreatic TME is often hypoxic owing to its desmoplastic stroma (37). Here, it was

found that coculture with adipocytes induced HIF-1α activity in PC cells. A previous study revealed that adipocytes could induce a glycolytic phenotype in prostate cancer via HIF-1α activation (38). Moreover, a recent study showed that HIF-1α signaling was activated by adipocyte-derived extracellular vesicles, and this functionally augmented the metastatic potential of breast cancer (39). The mechanisms by which adipocytes regulate HIF-1α expression in tumors remain elusive. One possible explanation is related to the fatty acids released by adipocytes. In liver cancer, OA treatment activated the FABP5/HIF-1α axis to promote cancer cell proliferation (40). Taken together, the present and previous studies highlight the potential role of adipocytes in the hypoxic TME and imply an intricate relationship between metabolic reprogramming and hypoxia in the adipocyte-PC cell coculture system.

Another finding of the present study was the energy-plundering relationship between PC cells and adipocytes. An increasing number of studies have confirmed the presence of lipid transfer from adipocytes to cancer cells (12-15). In the present study, coculturing with adipocytes led to increased mRNA levels of the fatty acid transport protein FATP1 and the LD protein PLIN-2 in cancer cells, suggesting a process of lipid transportation and storage in cocultured cancer cells. In line with this, the PC cells induced a decrease in LDs in adipocytes. Another key concern arising from the present study was that the increased amount of stored lipids in the cocultured PC cells contributed to cell invasion. The pharmacological inhibition of lipolysis or lipid transport into the mitochondria effectively hampered the invasive ability. Previous studies have shown that the demand for oxidative phosphorylation and ATP is increased in invasive and metastatic cancer cells (41-44); however, the source of this required energy has not been well defined. Intriguingly, recent work has demonstrated that in PC cells, excess lipids are required for ATP production to fuel the process of metastasis (27); in an elegant study, the oncogene KRAS was shown to facilitate the storage of LDs by suppressing hormone-sensitive lipase (HSL) expression, and stored lipids were then shown to be catabolized and utilized for tumor progression (27). The results of the present study indicated that adipocyte-derived lipids could be stored in cancer cells and utilized during invasion.

There remain some limitations to the present study. First, the findings were only confirmed at the cellular level, and need to be further verified using *in vivo* experiments. Second, in this study, the focus was primarily on the migration and invasion of PC cells. Certain other phenotypes of cancer cells, such as proliferation, chemoresistance, and immunoregulation, need to be further investigated. Third, the specific mechanisms of lipid transfer from adipocytes to PC cells were not revealed. Fourth, the characteristics of PC cells close to adipocytes in clinical specimens were not determined, for which, further research in combination with technologies such as space transcriptome sequencing is required to assess this. Fifth, only metabolic crosstalk has been observed in this study. Certain well-known adipocyte-secreting factors that may drive PC progression should be further elucidated. The types of cytokines mediating this process and their specific mechanisms need to be further studied.

In conclusion, these findings reveal a previously unidentified metabolic interaction between PC cells and adipocytes, leading to excess lipid storage and the priming of cancer cells for progression. Based on these results, interrupting the mechanisms of lipid uptake from adipocytes in the microenvironment may offer a potential strategy for attenuating PC metastasis.

Acknowledgements

We would like to thank Dr Abousalam Abdoulkader Ahmed from The Huadong Hospital Affiliated to Fudan University for his guidance in the development of this manuscript.

Funding

This study was supported by the Shanghai Science and Technology Commission of Shanghai Municipality (grant no. 20Y11908600), the Shanghai Shenkang Hospital Development Center (grant no. SHDC2020CR5008), the Shanghai Municipal Health Commission (grant no. 20194Y0195), and the Project of Huadong Hospital Affiliated to Fudan University (grant no. 2019H1285).

Availability of data and materials

The sequencing data have been deposited in the Gene Expression Omnibus with the assigned accession number GSE123939 (https://www.ncbi.nlm.nih.gov/geo/query/acc.cgi?acc=GSE123939). The datasets used and/or analyzed during the current study are available from the corresponding author on reasonable request.

Authors' contributions

ZC and CJ participated in the design of the study. ZC and YL performed data analysis and prepared the figures. MM, LW, HW, and ML participated in the analysis of the figures and data. ZC and YL prepared and revised the manuscript. CJ reviewed the results and revised the manuscript. ZC, YL and CJ confirm the authenticity of all the raw data. All authors have read and approved the final version of this manuscript.

Ethics approval and consent to participate

This study was approved by the Institutional Research Ethics Committee of Huadong Hospital, Fudan University (approval no. 2018K098). Written informed consent for the use of the tissue for scientific research was obtained from all patients.

Patient consent for publication

Not applicable.

Competing interests

The authors declare that they have no competing interests.

References

1. Mizrahi JD, Surana R, Valle JW and Shroff RT: Pancreatic cancer. Lancet 395: 2008-2020, 2020.
2. Sahai E: Illuminating the metastatic process. Nat Rev Cancer 7: 737-749, 2007.
3. Feig C, Gopinathan A, Neesse A, Chan DS, Cook N and Tuveson DA: The pancreas cancer microenvironment. Clin Cancer Res 18: 4266-4276, 2012.

4. Klein AP: Pancreatic cancer epidemiology: Understanding the role of lifestyle and inherited risk factors. Nat Rev Gastroenterol Hepatol 18: 493-502, 2021.
5. Chung KM, Singh J, Lawres L, Dorans KJ, Garcia C, Burkhardt DB, Robbins R, Bhutkar A, Cardone R, Zhao X, *et al*: Endocrine-Exocrine signaling drives obesity-associated pancreatic ductal adenocarcinoma. Cell 181: 832-847.e18, 2020.
6. Okumura T, Ohuchida K, Sada M, Abe T, Endo S, Koikawa K, Iwamoto C, Miura D, Mizuuchi Y, Moriyama T, *et al*: Extra-pancreatic invasion induces lipolytic and fibrotic changes in the adipose microenvironment, with released fatty acids enhancing the invasiveness of pancreatic cancer cells. Oncotarget 8: 18280-18295, 2017.
7. Hori M, Takahashi M, Hiraoka N, Yamaji T, Mutoh M, Ishigamori R, Furuta K, Okusaka T, Shimada K, Kosuge T, *et al*: Association of pancreatic Fatty infiltration with pancreatic ductal adenocarcinoma. Clin Transl Gastroenterol 5: e53, 2014.
8. Incio J, Liu H, Suboj P, Chin SM, Chen IX, Pinter M, Ng MR, Nia HT, Grahovac J, Kao S, *et al*: Obesity-induced inflammation and desmoplasia promote pancreatic cancer progression and resistance to chemotherapy. Cancer Discov 6: 852-869, 2016.
9. Quail DF and Dannenberg AJ: The obese adipose tissue microenvironment in cancer development and progression. Nat Rev Endocrinol 15: 139-154, 2019.
10. O'Sullivan J, Lysaght J, Donohoe CL and Reynolds JV: Obesity and gastrointestinal cancer: The interrelationship of adipose and tumour microenvironments. Nat Rev Gastroenterol Hepatol 15: 699-714, 2018.
11. Cai Z, Liang Y, Xing C, Wang H, Hu P, Li J, Huang H, Wang W and Jiang C*:* Cancer-associated adipocytes exhibit distinct phenotypes and facilitate tumor progression in pancreatic cancer. Oncol Rep 42: 2537-2549, 2019.
12. Wang YY, Attané C, Milhas D, Dirat B, Dauvillier S, Guerard A, Gilhodes J, Lazar I, Alet N, Laurent V, *et al*: Mammary adipocytes stimulate breast cancer invasion through metabolic remodeling of tumor cells. JCI Insight 2: e87489, 2017.
13. Nieman KM, Kenny HA, Penicka CV, Ladanyi A, Buell-Gutbrod R, Zillhardt MR, Romero IL, Carey MS, Mills GB, Hotamisligil GS, *et al*: Adipocytes promote ovarian cancer metastasis and provide energy for rapid tumor growth. Nat Med 17: 1498-1503, 2011.
14. Zhang M, Di Martino JS, Bowman RL, Campbell NR, Baksh SC, Simon-Vermot T, Kim IS, Haldeman P, Mondal C, Yong-Gonzales V, *et al*: Adipocyte-derived lipids mediate melanoma progression via FATP proteins. Cancer Discov 8: 1006-1025, 2018.
15. Wen YA, Xing X, Harris JW, Zaytseva YY, Mitov MI, Napier DL, Weiss HL, Mark Evers B and Gao T: Adipocytes activate mitochondrial fatty acid oxidation and autophagy to promote tumor growth in colon cancer. Cell Death Dis 8: e2593, 2017.
16. Qian SW, Tang Y, Li X, Liu Y, Zhang YY, Huang HY, Xue RD, Yu HY, Guo L, Gao HD, *et al*: BMP4-mediated brown fat-like changes in white adipose tissue alter glucose and energy homeostasis. Proc Natl Acad Sci USA 110: E798-E807, 2013.
17. Takehara M, Sato Y, Kimura T, Noda K, Miyamoto H, Fujino Y, Miyoshi J, Nakamura F, Wada H, Bando Y, *et al*: Cancer-associated adipocytes promote pancreatic cancer progression through SAA1 expression. Cancer Sci 111: 2883-2894, 2020.
18. Livak KJ and Schmittgen TD: Analysis of relative gene expression data using real-time quantitative PCR and the 2(-Delta Delta C(T)) method. Methods 25: 402-408, 2001.
19. Zhou B, Wu D, Liu H, Du LT, Wang YS, Xu JW, Qiu FB, Hu SY and Zhan HX: Obesity and pancreatic cancer: An update of epidemiological evidence and molecular mechanisms. Pancreatology 19: 941-950, 2019.
20. Shuff S, Oyama Y, Walker L and Eckle T: Circadian Angiopoietin-Like-4 as a Novel Therapy in Cardiovascular Disease. Trends Mol Med 27: 627-629, 2021.
21. Qiao G, Wu A, Chen X, Tian Y and Lin X: Enolase 1, a moonlighting protein, as a potential target for cancer treatment. Int J Biol Sci 17: 3981-3992, 2021.
22. Sharma D, Singh M and Rani R: Role of LDH in tumor glycolysis: Regulation of LDHA by small molecules for cancer therapeutics. Semin Cancer Biol 87: 184-195, 2022.
23. Pedroso JAB, Ramos-Lobo AM and Donato J Jr: SOCS3 as a future target to treat metabolic disorders. Hormones (Athens) 18: 127-136, 2019.
24. Wunderlich CM, Hövelmeyer N and Wunderlich FT: Mechanisms of chronic JAK-STAT3-SOCS3 signaling in obesity. Jakstat 2: e23878, 2013.
25. Wang T, Fahrmann JF, Lee H, Li YJ, Tripathi SC, Yue C, Zhang C, Lifshitz V, Song J, Yuan Y, *et al*: JAK/STAT3-regulated Fatty acid β-oxidation is critical for breast cancer stem cell self-renewal and chemoresistance. Cell Metab 27: 136-150.e5, 2018.
26. Garcia D and Shaw RJ: AMPK: Mechanisms of cellular energy sensing and restoration of metabolic balance. Mol Cell 66: 789-800, 2017.
27. Rozeveld CN, Johnson KM, Zhang L and Razidlo GL: KRAS controls pancreatic cancer cell lipid metabolism and invasive potential through the lipase HSL. Cancer Res 80: 4932-4945, 2020.
28. Dumas JF and Brisson L: Interaction between adipose tissue and cancer cells: Role for cancer progression. Cancer Metastasis Rev 40: 31-46, 2021.
29. Lyssiotis CA and Kimmelman AC: Metabolic Interactions in the tumor microenvironment. Trends Cell Biol 27: 863-875, 2017.
30. Mukherjee A, Chiang CY, Daifotis HA, Nieman KM, Fahrmann JF, Lastra RR, Romero IL, Fiehn O and Lengyel E: Adipocyte-induced FABP4 expression in ovarian cancer cells promotes metastasis and mediates carboplatin resistance. Cancer Res 80: 1748-1761, 2020.
31. Ye H, Adane B, Khan N, Sullivan T, Minhajuddin M, Gasparetto M, Stevens B, Pei S, Balys M, Ashton JM, *et al*: Leukemic stem cells evade chemotherapy by metabolic adaptation to an adipose tissue niche. Cell Stem Cell 19: 23-37, 2016.
32. Andersen DK, Korc M, Petersen GM, Eibl G, Li D, Rickels MR, Chari ST and Abbruzzese JL: Diabetes, pancreatogenic diabetes, and pancreatic cancer. Diabetes 66: 1103-1110, 2017.
33. Permert J, Ihse I, Jorfeldt L, von Schenck H, Arnquist HJ and Larsson J: Improved glucose metabolism after subtotal pancreatectomy for pancreatic cancer. Br J Surg 80: 1047-1050, 1993.
34. Pannala R, Basu A, Petersen GM and Chari ST: New-onset diabetes: A potential clue to the early diagnosis of pancreatic cancer. Lancet Oncol 10: 88-95, 2009.
35. Basso D, Brigato L, Veronesi A, Panozzo MP, Amadori A and Plebani M: The pancreatic cancer cell line MIA PaCa2 produces one or more factors able to induce hyperglycemia in SCID mice. Anticancer Res 15: 2585-2588, 1995.
36. Moldogazieva NT, Mokhosoev IM and Terentiev AA: Metabolic heterogeneity of cancer cells: An Interplay between HIF-1, GLUTs, and AMPK. Cancers (Basel) 12: 862, 2020.
37. Fuentes NR, Phan J, Huang Y, Lin D and Taniguchi CM: Resolving the HIF paradox in pancreatic cancer. Cancer Lett 489: 50-55, 2020.
38. Diedrich JD, Rajagurubandara E, Herroon MK, Mahapatra G, Hüttemann M and Podgorski I: Bone marrow adipocytes promote the Warburg phenotype in metastatic prostate tumors via HIF-1α activation. Oncotarget 7: 64854-64877, 2016.
39. La Camera G, Gelsomino L, Malivindi R, Barone I, Panza S, De Rose D, Giordano F, D'Esposito V, Formisano P, Bonofiglio D,*et al*: Adipocyte-derived extracellular vesicles promote breast cancer cell malignancy through HIF-1α activity. Cancer Lett 521: 155-168, 2021.
40. Seo J, Jeong DW, Park JW, Lee KW, Fukuda J and Chun YS: Fatty-acid-induced FABP5/HIF-1 reprograms lipid metabolism and enhances the proliferation of liver cancer cells. Commun Biol 3: 638, 2020.
41. Cunniff B, McKenzie AJ, Heintz NH and Howe AK: AMPK activity regulates trafficking of mitochondria to the leading edge during cell migration and matrix invasion. Mol Biol Cell 27: 2662-2674, 2016.
42. Lin S, Huang C, Gunda V, Sun J, Chellappan SP, Li Z, Izumi V, Fang B, Koomen J, Singh PK, *et al*: Fascin controls metastatic colonization and mitochondrial oxidative phosphorylation by remodeling mitochondrial actin filaments. Cell Rep 28: 2824-2836.e8, 2019.
43. LeBleu VS, O'Connell JT, Gonzalez Herrera KN, Wikman H, Pantel K, Haigis MC, de Carvalho FM, Damascena A, Domingos Chinen LT, Rocha RM, *et al*: PGC-1α mediates mitochondrial biogenesis and oxidative phosphorylation in cancer cells to promote metastasis. Nat Cell Biol 16: 992-1003, 2014.
44. Kelley LC, Chi Q, Cáceres R, Hastie E, Schindler AJ, Jiang Y, Matus DQ, Plastino J and Sherwood DR: Adaptive F-actin polymerization and localized ATP production drive basement membrane invasion in the absence of MMPs. Dev Cell 48: 313-328.e8, 2019.